Methanol Dehydrogenation and Oxidation on Pt(111) in Alkaline Solutions†

Jacob S. Spendelow,‡ Jason D. Goodpaster, Paul J. A. Kenis, and Andrzej Wieckowski*

Department of Chemistry and Department of Chemical and Biomolecular Engineering, University of Illinois at Urbana−Champaign, 600 South Mathews Avenue, Urbana, Illinois 61801

Received June 2, 2006. In Final Form: August 17, 2006

Adsorption, dehydrogenation, and oxidation of methanol on Pt(111) in alkaline solutions has been examined from a fundamental mechanistic perspective, focusing on the role of adsorbate−adsorbate interactions and the effect of defects on reactivity. CO has been confirmed as the main poisoning species, affecting the rate of methanol dehydrogenation primarily through repulsive interactions with methanol dehydrogenation intermediates. At direct methanol fuel cell (DMFC)-relevant potentials, methanol oxidation occurs almost entirely through a CO intermediate, and the rate of CO oxidation is the main limiting factor in methanol oxidation. Small Pt island defects greatly enhance CO oxidation, though they are effective only when the CO coverage is 0.20 ML or higher. Large Pt islands enhance CO oxidation as well, but unlike small Pt islands, they also promote methanol dehydrogenation. Perturbations in electronic structure are responsible for the CO oxidation effect of defects, but the role of large Pt islands in promoting methanol dehydrogenation is primarily explained by surface geometric structure.

1. Introduction

Mechanisms of adsorption, decomposition, and oxidation of methanol on Pt-based surfaces are of practical interest because of the numerous advantages of methanol as a fuel in direct methanol fuel cells (DMFCs).[1,2] Most experimental studies of methanol oxidation to date have been performed with acidic electrolytes, but some studies have also been performed in alkaline electrolytes, including several studies within the past three years.[3−8] At the same time, progress has been made in alkaline DMFC development. Notably, in the past two years, significant improvements have been made in the performance of fuel-flexible, media-flexible, laminar flow fuel cells,[9−11] along with advances in anion-exchange membranes for alkaline fuel cells.[12−16]

Poor electrocatalytic activity for methanol oxidation continues to constrain the development of alkaline DMFCs. Although recent reports have demonstrated that Pt-based catalysts have higher activity for methanol oxidation in alkaline media than in acidic media,[11,17,18] further improvement is needed in order to allow the catalyst loading to be decreased to economically viable levels. To that end, we have performed a series of fundamental studies of anode electrocatalysis on clean and Ru-modified Pt single crystals in alkaline solutions, including previously published work on CO oxidation,[19,20] as well as work on methanol oxidation.[21]

The goal of this work is to develop an understanding of the mechanisms and limiting factors in alkaline anode electrocatalysis, including the roles of defect sites and of admetal promoters on methanol dehydrogenation and CO oxidation. Similar to results from acidic media,[22] we have found that defects are the active sites in CO oxidation on Pt(111) at DMFC-relevant potentials in alkaline media, since the OH adsorbate required for CO oxidation does not form on terraces below 0.65 V. The role of CO and OH adsorption strength is of pivotal importance, since strong CO adsorption at low coverage makes CO unreactive with defect-bound OH.[20] Thus, at low CO coverage, CO can only be oxidized by the terrace-bound OH that forms at high potential. Since the CO coverage is rather low during methanol oxidation on Pt(111) in alkaline media, this coverage-dependent reactivity has significant implications for CO removal during methanol oxidation. In the present work, particular attention is given to the effect of adsorbate−adsorbate interactions in determining rates of methanol dehydrogenation and CO oxidation, as well as to the different roles of terrace sites, step-type defects, and kink-type defects on these reactions. The new mechanistic discoveries and interpretations presented here are important steps in the understanding of fundamental electrocatalytic processes,

† Part of the Electrochemistry special issue.

* Corresponding author: Tel.: +1-217-333-7943. Fax: +1-217-244-8068. E-mail: andrzej@scs.uiuc.edu.

‡ Present address: MPA-11, MS D429, Los Alamos National Laboratory, PO Box 1663, Los Alamos, NM 87545.

(1) McNicol, B. D.; Rand, D. A. J.; Williams, K. R. *J. Power Sources* **1999**, *83*, 15.
(2) Dillon, R.; Srinivasan, S.; Arico, A. S.; Antonucci, V. *J. Power Sources* **2004**, *127*, 112.
(3) Luo, J.; Njoki, P. N.; Lin, Y.; Mott, D.; Wang, L. Y.; Zhong, C. J. *Langmuir* **2006**, *22*, 2892.
(4) Shen, P. K.; Xu, C. W.; Zeng, R.; Liu, Y. L. *Electrochem. Solid State Lett.* **2006**, *9*, A39.
(5) Nishihara, C.; Okada, T. *J. Electroanal. Chem.* **2005**, *577*, 355.
(6) Hoor, F. S.; Ahmed, M. F.; Mayanna, S. M. *J. Solid State Electrochem.* **2004**, *8*, 572.
(7) Yu, E. H.; Scott, K.; Reeve, R. W. *J. Electroanal. Chem.* **2003**, *547*, 17.
(8) Tripkovic, A. V.; Strabac, S.; Popovic, K. D. *Electrochem. Commun.* **2003**, *5*, 484.
(9) Choban, E. R.; Spendelow, J. S.; Gancs, L.; Wieckowski, A.; Kenis, P. J. A. *Electrochim. Acta* **2005**, *50*, 5390.
(10) Jayashree, R. S.; Gancs, L.; Choban, E. R.; Primak, A.; Natarajan, D.; Markoski, L. J.; Kenis, P. J. A. *J. Am. Chem. Soc.* **2005**, *127*, 16758.
(11) Jayashree, R. S.; Egas, D.; Spendelow, J. S.; Natarajan, D.; Markoski, L. J.; Kenis, P. J. A. *Electrochem. Solid State Lett.* **2006**, *9*, A252.
(12) Huang, A. B.; Xia, C. Y.; Xiao, C. B.; Zhuang, L. *J. Appl. Polym. Sci.* **2006**, *100*, 2248.
(13) Matsuoka, K.; Iriyama, Y.; Abe, T.; Matsuoka, M.; Ogumi, Z. *J. Power Sources* **2005**, *150*, 27.
(14) Li, L.; Wang, Y. X. *J. Membr. Sci.* **2005**, *262*, 1.
(15) Varcoe, J. R.; Slade, R. C. T. *Fuel Cells* **2005**, *5*, 187.
(16) Yu, E. H.; Scott, K. *J. Appl. Electrochem.* **2005**, *35*, 91.
(17) Tripkovic, A. V.; Popovic, K. D.; Grgur, B. N.; Blizanac, B.; Ross, P. N.; Markovic, N. M. *Electrochim. Acta* **2002**, *47*, 3707.
(18) Prabhuram, J.; Manoharan, R. *J. Power Sources* **1998**, *74*, 54.
(19) Spendelow, J. S.; Lu, G. Q.; Kenis, P. J. K.; Wieckowski, A. *J. Electroanal. Chem.* **2004**, *568*, 215.
(20) Spendelow, J. S.; Goodpaster, J. D.; Kenis, P. J. A.; Wieckowski, A. *J. Phys. Chem. B* **2006**, *110*, 9545.
(21) Spendelow, J. S.; Goodpaster, J. D.; Johnston, C. M.; Kenis, P. J. A.; Wieckowski, A. in preparation.
(22) Lebedeva, N. P.; Koper, M. T. M.; Feliu, J. M.; van Santen, R. A. *J. Electroanal. Chem.* **2002**, *524*, 242.

10.1021/la0615995 CCC: $33.50
Published on Web 09/27/2006

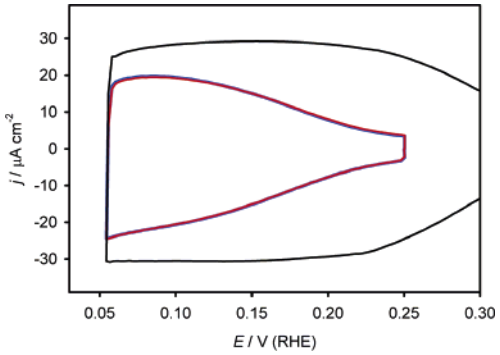

Figure 1. Cyclic voltammetry in the H adsorption region on a Pt(111) electrode previously held at 0.45 V in 0.1 M CH_3OH + 0.1 M NaOH solution for 10 min. Blue line, in methanol solution; red line, after transfer to methanol free solution; black line, after voltammetric CO stripping.

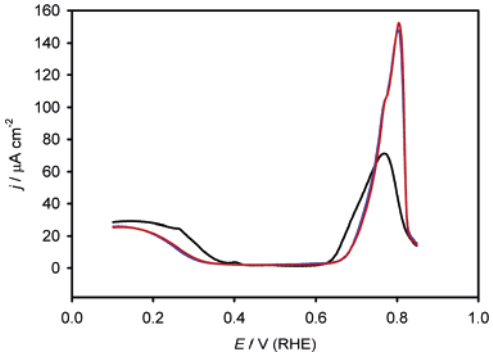

Figure 2. Subsaturated CO stripping voltammograms. Blue line, 0.12 ML CO produced by dosing of gas-phase CO followed by Ar purging to remove dissolved CO; red line, 0.12 ML CO produced by oxidation of 0.1 M methanol at 0.35 V for 30 s; black line, background voltammogram.

as well as in the development of alkaline DMFCs with high power density and high efficiency.

2. Experimental Section

All experiments were performed with either a 2-mm bead-type Pt(111) electrode or a 3-mm cylindrical Pt(111) electrode. Materials used were Ar and H_2 (SJ Smith, ultrahigh purity), CO (SJ Smith, research grade), H_2SO_4 (GFS, double distilled from Vycor), and NaOH (Merck, suprapur). Electrochemical measurements were performed in a two-compartment cell with a Pt wire counter electrode and a Ag/AgCl reference electrode (BAS, $[Cl^-] = 3$ M), although all potentials are quoted on the RHE scale. An Autolab PGSTAT 30 potentiostat was used for all measurements. Full experimental details are given elsewhere.[20] Briefly, the clean electrode was annealed in a H_2 flame and cooled in H_2 + Ar then covered with a drop of H_2-saturated water for transfer to the electrochemical cell. After potential cycling in 0.1 M H_2SO_4, the electrode was rinsed with Ar-purged water and the solution was replaced with 0.1 M NaOH, all under a continuous Ar blanket. Adsorption of CO was performed by replacing the Ar blanketing gas with a ~5% CO/~95% Ar stream while the electrode was maintained in meniscus configuration at a potential of 0.10 V. Ar-purged methanol was added to the solution using a glass and PTFE syringe through a PTFE needle inserted into the cell from the top. After methanol oxidation, the CO coverage was measured by emersing the electrode, rinsing with NaOH solution, and immersing in methanol-free 0.1 M NaOH (all under an Ar blanket). As long as the Ar flow rate is large enough, no changes in the H UPD region can be detected during this procedure (Figure 1). These results demonstrate that no significant changes in the adsorbed CO layer occur during the transfer to methanol-free solution, validating the solution-exchange approach to the study of methanol oxidation intermediates. For experiments in which the most precise CO coverage measurement is necessary, e.g., measuring coverages of CO under 0.05 ML, a small amount of H_2 gas was fed into the Ar blanketing stream during solution exchange to ensure that methanol dehydrogenation and CO oxidation were completely stopped before and during the solution exchange. All potential scan rates are 50 mV s^{-1}. Error estimates are based on 95% confidence intervals.

3. Results and Discussion

3.1. Sources of Methanol Current Decay. Methanol decomposition to CO proceeds efficiently on Pt surfaces,[23−26] but the rapidly increasing CO coverage inhibits further methanol adsorption and decomposition. Although CO has been widely reported as a poisoning intermediate during methanol oxidation on Pt-based surfaces in acidic electrolytes,[27−29] several reports of surprisingly small CO absorption bands in FTIR spectra recorded during methanol oxidation on Pt(111) in alkaline electrolytes[30,31] have caused some workers to conclude that CO formation is negligible during methanol oxidation on Pt(111) in alkaline media.[31,32] Instead, a significant role of alternative methanol oxidation intermediates, such as HCO, has been proposed.[32,33] Although species such as HCO or COH exist as transient intermediates during the oxidation of methanol to CO or formate, the results displayed in Figure 2 demonstrate that, on the typical experimental time scale, the coverage of these intermediates is much lower than that of CO. The cyclic voltammograms in Figure 2 correspond to Pt(111) surfaces with CO adlayers formed by methanol decomposition (red line) and by exposure of the clean electrode to dissolved CO (blue line). Comparison of the two voltammograms, which are identical, leads to our conclusion that CO is the main nontransient adsorbed intermediate during methanol oxidation in alkaline electrolytes.

The current−time decay during methanol oxidation, depicted in Figure 3, is primarily caused by CO poisoning. This interpretation is supported by the CO coverage vs time results summarized in Figure 4. At 0.45 V, the methanol oxidation current levels off at a steady-state value of 0.41 ± 0.05 μA cm^{-2} after ~300 s. The time required to reach this steady-state value agrees very well with the time required to reach the steady-state CO coverage (Figure 4). The results at 0.55 V are somewhat different. Despite the negative correlation between CO coverage and methanol oxidation current, the decay in the 0.55 V chronoamperogram (Figure 3) at long times cannot be explained entirely by increasing CO coverage, since the decay continues even after the CO coverage has reached steady state. We have further confirmed that the decay at long times is not caused by increasing CO coverage by examining methanol oxidation on surfaces pre-

(23) Lu, G. Q.; Chrzanowski, W.; Wieckowski, A. *J. Phys. Chem. B* **2000**, *104*, 5566.
(24) Franaszczuk, K.; Herrero, E.; Zelenay, P.; Wieckowski, A.; Wang, J.; Masel, R. I. *J. Phys. Chem.* **1992**, *96*, 8509.
(25) Herrero, E.; Franaszczuk, K.; Wieckowski, A. *J. Phys. Chem.* **1994**, *98*, 5074.
(26) Cao, D.; Lu, G. Q.; Wieckowski, A.; Wasileski, S. A.; Neurock, M. *J. Phys. Chem. B* **2005**, *109*, 11622.
(27) Parsons, R.; Vandernoot, T. *J. Electroanal. Chem.* **1988**, *257*, 9.
(28) Hamnett, A. Mechanism of Methanol Electro-Oxidation. In *Interfacial Electrochemistry: Theory, Experiment, and Applications*; Wieckowski, A., Ed.; Marcel Dekker: New York, 1999; p 843.
(29) Iwasita, T. *Electrochim. Acta* **2002**, *47*, 3663.
(30) Morallon, E.; Rodes, A.; Vazquez, J. L.; Perez, J. M. *J. Electroanal. Chem.* **1995**, *391*, 149.
(31) Tripkovic, A. V.; Marinkovic, N.; Popovic, K. D.; Adzic, R. R. *Russ. J. Electrochem.* **1995**, *31*, 993.
(32) Tripkovic, A. V.; Popovic, K. D.; Momcilovic, J. D.; Drazic, D. M. *J. Electroanal. Chem.* **1996**, *418*, 9.
(33) Tripkovic, A. V.; Popovic, K. D.; Lovic, J. D.; Jovanovic, V. M.; Kowal, A. *J. Electroanal. Chem.* **2004**, *572*, 119.

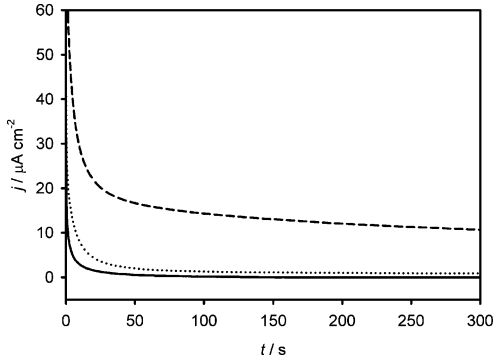

Figure 3. Oxidation of 0.1 M CH_3OH in 0.1 M NaOH. Solid line, 0.35 V; dotted line: 0.45 V; dashed line, 0.55 V.

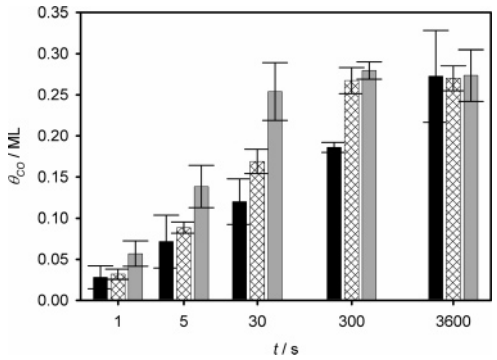

Figure 4. CO coverage after 1, 5, 30, 300, and 3600 s in 0.1 M CH_3OH + 0.1 M NaOH. Black, 0.35 V; crosshatch, 0.45 V; gray, 0.55 V.

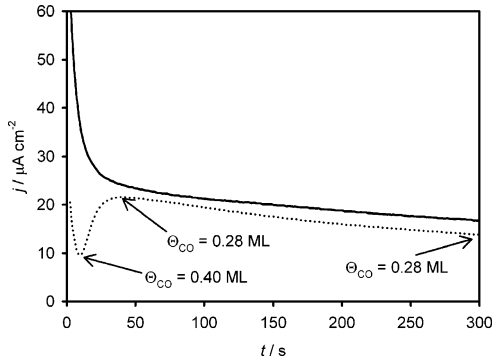

Figure 5. Oxidation of methanol at 0.55 V on initially clean Pt-(111) (solid line) and CO presaturated Pt(111) (dotted line). The CO presaturated surface was prepared by dosing CO gas followed by Ar purging to remove dissolved CO from the solution.

covered with a saturated CO adlayer by dosing of CO gas (Figure 5). On these surfaces, an initial decay is observed, corresponding to the CO oxidation current transient.[19,20] The current reaches a minimum and then increases as enough Pt sites are opened to allow methanol oxidation to occur. The current then reaches a maximum value before beginning a slow decay, essentially identical to the decay observed during methanol oxidation without CO presaturation. Since the adsorbed CO formed by dosing of CO gas has properties similar to those of CO formed by methanol oxidation (as demonstrated by Figure 2) and since the rate of CO oxidation increases monotonically with the CO coverage,[20] while the rate of CO formation from methanol decreases monotonically with increasing CO coverage (Figure 4), the CO coverage can only decrease during the experiment illustrated in Figure 5. Therefore, the slow decay beginning around $t = 40$ s in Figure 5 cannot be explained by increasing CO coverage. At present, the cause of this slow decay is uncertain, though we have observed

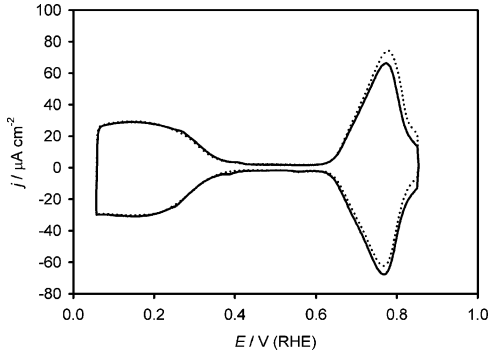

Figure 6. Pt(111) cyclic voltammogram in 0.1 M NaOH (solid line) and 0.01 M NaHCOO + 0.1 M NaOH (dotted line).

that the methanol oxidation current can be almost completely restored to the pre-decay value by stepping the potential to 0.10 V and holding for several seconds before stepping back to the working potential. Therefore, the slow decay could be caused by specific adsorption of an anionic species that adsorbs at potentials higher than 0.10 V, although the nature of this hypothetical species is unresolved. Formate, produced as a major product during methanol oxidation in alkaline media,[30] may be excluded, since cyclic voltammograms recorded in solutions containing 0.01 M NaHCOO reveal negligible formate adsorption below 0.70 V (Figure 6). Carbonate, which adsorbs in the same potential range as formate,[32] has similarly been excluded. Alternatively, the reversal of the current decay that occurs after a step to 0.10 V could be caused by adsorption of H at low potentials. Since coadsorbed H and CO are known to interact repulsively on Pt(111), leading to segregation of CO and H into separate islands under UHV conditions,[34,35] a step to 0.10 V could similarly modify the CO surface distribution under electrochemical conditions. Redistribution of surface CO into islands would be expected to increase the rate of CO oxidation, as a result of lateral CO−CO repulsion.[20] Similarly, such a CO redistribution would lead to an increased rate of methanol dehydrogenation since it would provide areas of the surface with a relatively low local CO coverage. This hypothetical role of the CO surface distribution in causing the slow methanol oxidation current decay at 0.55 V is consistent with previous studies that have detected a nonuniform CO distribution during oxidation of CO,[36] as well as methanol.[37,38] Therefore, the observed reversal of the slow current decay following a step to 0.10 V could be consistent with either an effect of anion desorption or H adsorption. Further work is required to achieve a better understanding of the mechanism of this decay.

3.2. Rates of Methanol Dehydrogenation and CO Oxidation. Previous workers have shown that the rate of CO formation on Pt in acidic methanol solutions can be modeled using the Elovich equation (eq 1), which assumes a linear dependence of the dehydrogenation activation barrier on CO coverage.[39,40]

$$\frac{d\theta_{CO}}{dt} = \frac{k_a C_m}{S} \exp(-\alpha\theta_{CO}) \qquad (1)$$

Parameters in eq 1 include the rate constants for methanol

(34) Wang, H.; Tobin, R. G.; Lamberg, D. K.; Fisher, G. B.; Dimaggio, C. L. *Surf. Sci.* **1995**, *330*, 173.
(35) Hoge, D.; Tushaus, M.; Bradshaw, A. M. *Surf. Sci.* **1988**, *207*, L935.
(36) Furuya, N.; Motoo, S.; Kunimatsu, K. *J. Electroanal. Chem.* **1988**, *239*, 347.
(37) Chang, S. C.; Leung, L. W. H.; Weaver, M. J. *J. Phys. Chem.* **1990**, *94*, 6013.
(38) Xia, X. H.; Iwasita, T.; Ge, F.; Vielstich, W. *Electrochim. Acta* **1996**, *41*, 711.

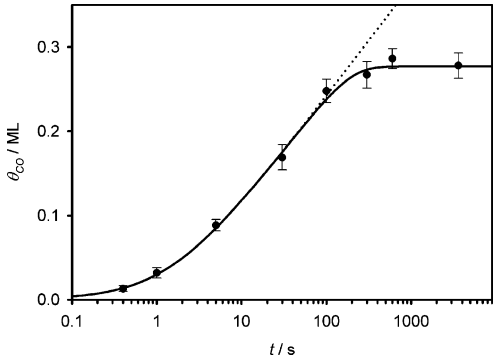

Figure 7. CO coverage vs time at 0.45 V in 0.1 M CH_3OH + 0.1 M NaOH. Circles, experimental data points; dotted line, fit of eq 2 to 0.4−100 s data, with parameter values $k_a = (1.0 \pm 0.2) \times 10^{-6}$ cm s^{-1}, $\alpha = 18 \pm 1$ ML^{-1}; solid line, numerical solution of eq 3 with $k_a = 1.0 \times 10^{-6}$ cm s^{-1}, $\alpha = 18$ ML^{-1}, $k_o = 1.9 \times 10^9$ molecules cm^{-2} s^{-1}, $\beta = 20$ ML^{-1} (k_o and β values from Figure 8).

dehydrogenation (k_a), the methanol concentration (C_m), and α, which represents the effect of repulsive CO interactions on the rate of methanol dehydrogenation. The constant S represents the density of surface sites, which is 1.5×10^{15} atoms cm^{-2}. Solving eq 1 with the initial condition $\theta_{CO} = 0$ yields eq 2:

$$\theta_{CO} = \frac{1}{\alpha} \ln\left(\frac{\alpha k_a C_m}{S} t + 1\right) \quad (2)$$

Equation 2 indicates that θ_{CO} should increase linearly with $\ln(t)$ for $t \gg S/(\alpha\, k_a C_m)$, in agreement with the quasi-linear behavior for 5 s < t < 100 s in Figure 7. Equation 2 was fit to the θ_{CO} vs time data for methanol oxidation at 0.45 V, producing a good fit for t < 100 s (Figure 7, dotted trace), but the model clearly cannot fit the behavior at longer times.

The asymptotic approach to a steady-state coverage shown by the experimental data points in Figure 7 implies that, at long times, the rates of CO generation and oxidation become equal. Therefore, oxidation of the methanol-generated CO at 0.45 V was further analyzed to determine the CO coverage dependence of the oxidation rate. After formation of the steady-state CO coverage by methanol oxidation at 0.45 V, the methanol solution was replaced by methanol-free solution and the potential was stepped repeatedly between 0.25 and 0.45 V to oxidize CO. Between CO oxidation steps, the potential was rapidly stepped between 0.20 and 0.35 V to determine the H UPD charge in this region, from which the CO coverage was calculated using the empirical correlation shown in Figure 8B. The correlation in Figure 8B does not have any physical significance; rather, it is simply a tool for determining CO coverage. A plot of CO oxidation rate vs CO coverage prepared by this method (Figure 8A) reveals an exponential relationship, in agreement with the predictions of a Frumkin isotherm, in which the activation barrier for CO oxidation varies linearly with θ_{CO}.[41] Therefore, an exponential CO oxidation term can be added to eq 1, yielding eq 3:

$$\frac{d\theta_{CO}}{dt} = \frac{k_a C_m}{S} \exp(-\alpha\theta_{CO}) - \frac{k_o}{S} \exp(\beta\theta_{CO}) \quad (3)$$

The new parameters in eq 3 are k_o, the rate constant for CO oxidation, and β, which represents the effect of repulsive CO interactions on the rate of CO oxidation. Values of k_a and α were

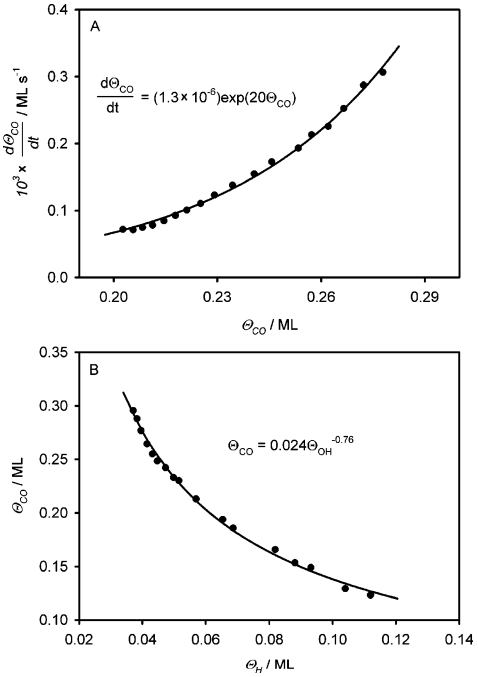

Figure 8. Oxidation of a CO adlayer prepared by methanol oxidation at 0.45 V for 400 s. (A) CO oxidation rate vs CO coverage, with fit of eq 3 ($C_m = 0$). Fitted parameter values: $k_o = (1.9 \pm 0.3) \times 10^9$ molecules cm^{-2} s^{-1}, $\beta = 20 \pm 1$ ML^{-1} (B) CO coverage (determined by CO stripping) vs H coverage between 0.20 and 0.35 V. The empirical correlation in (B), $\theta_{CO} = 0.024\theta_H^{-0.76}$, was used to calculate CO coverage in (A).

obtained from the fit in Figure 7 (dotted trace), while values of k_o and β were obtained from the fit in Figure 8A. Numerical solution of eq 3 produces a θ_{CO} vs t curve that matches the data well (Figure 7, solid line), most notably in the excellent agreement between the calculated and measured steady-state CO coverage (t > 300 s). The good agreement between eq 3 and the data suggests that Frumkin effects are dominant during methanol dehydrogenation and oxidation. Nevertheless, the addition of a site-blocking term to the model equation was also considered. With the site-blocking term, the model may be written as eq 4.

$$\frac{d\theta_{CO}}{dt} = \frac{k_a C_m}{S} \exp(-\alpha\theta_{CO})(1 - \theta_{CO})^y - \frac{k_o}{S} \exp(\beta\theta_{CO}) \quad (4)$$

Equation 4 contains an additional fitting parameter, y. Using an F-test, we found that the addition of site-blocking effects to the model does not significantly improve the fit, with eq 4 determined to be a better model than eq 3 only at the 10% confidence level. The ability to fit the data well without any site blocking term indicates that CO poisoning is primarily characterized by repulsive interactions between CO and adsorbed methanol, i.e., the effect of CO on the activation barrier for methanol dehydrogenation is much more significant than the effect of blocking methanol adsorption sites.

The validity of eq 3 and the fitted parameter values were further verified by examining the effect of methanol concentration on the steady-state CO coverage at 0.45 V. At steady-state, eq 3 can be rearranged and differentiated to arrive at eq 5:

$$\frac{d\theta_{CO}}{d \log C_m} = \frac{2.303}{\alpha + \beta} \quad (5)$$

Substituting in the fitted values, $\alpha = 18 \pm 1$ and $\beta = 20 \pm 1$, yields an expected change in CO coverage of 0.061 ± 0.002

(39) Khazova, O. A.; Mikhailova, A. A.; Skundin, A. M.; Tuseeva, E. K.; Havránek, A.; Wippermann, K. *Fuel Cells* **2002**, *2*, 99.
(40) Seiler, T.; Savinova, E. R.; Friedrich, K. A.; Stimming, U. *Electrochim. Acta* **2004**, *49*, 3927.
(41) Gileadi, E. *Electrode Kinetics*; VCH: New York, 1993.

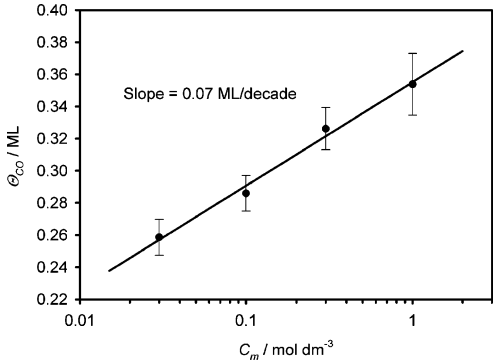

Figure 9. Steady-state CO coverage after 600 s at 0.45 V vs methanol concentration.

ML per decade change in concentration. This is in good agreement with the measured value of 0.07 ± 0.02 ML per decade (Figure 9), further confirming the validity of the model (eq 3) and the values of α and β.

3.3. Mechanism of Methanol Dehydrogenation. The dependence of reaction rate on potential provides information about the mechanism and rate-limiting step of methanol dehydrogenation. We measured the Tafel slope at various values of the CO coverage by holding the potential at 0.55 V in methanol-containing solution to generate the desired CO coverage, followed by holding the potential at 0.10 V for 5 s, then stepping to 0.24 V for 2 s, followed by a step to the final potential. The initial current at this potential (after decay of capacitive currents) was used in calculating the Tafel slope. Using this method for a CO coverage of 0.15 ML, the Tafel slope at 0.52 V and higher was found to be 120 mV decade^{-1}, while at potentials below 0.35 V, the Tafel slope was 100 mV decade^{-1} (Figure 10). The intermediate region is characterized by a Tafel slope of 200−300 mV decade^{-1} and reflects the existence of more than one slow step, which will be elaborated upon below. Qualitatively similar results were obtained at θ_{CO} = 0.04 and 0.09 ML.

Methanol dehydrogenation to CO is a stepwise process, involving scission of three C−H bonds and one O−H bond. The order in which these bonds are broken is not yet known, although experiments with CD_3OH,[24] as well as quantum chemical calculations,[42] indicate that the first step involves scission of a C−H bond. On the basis of our Tafel analysis, it appears that more than one step is rate limiting. Although we cannot identify exactly which steps are rate limiting, for the purpose of the discussion, abstraction of the first and fourth H atoms will be assumed to be the slow steps. This assignment is made in consideration of evidence to support rate-limiting scission of the first C−H bond,[23,24,43−45] as well as reports indicating that COH and/or CHO may be at least sparingly stable on Pt(111).[38,46,47]

At low potential, the Tafel slope of 100 mV decade^{-1} is close to the expected value of 120 mV decade^{-1} for a first electron transfer rate limiting step and likely reflects slow scission of the first C−H bond. In this low-potential regime (below 0.35 V), further oxidation to CHO or COH would likely be rapid,[48] but

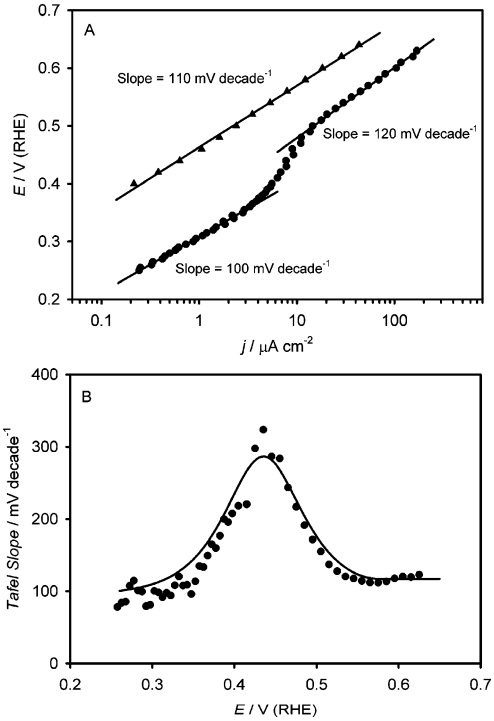

Figure 10. (A) Tafel plots for oxidation of 0.1 M CH_3OH in 0.1 M NaOH. Circles, surface precovered with 0.15 ML of CO; triangles, surface precovered with quasi-steady-state CO coverage (~0.28 ML). (B) Tafel slope vs potential for surface precovered with 0.15 ML CO. Circles, experimental data points; solid line, simulated data. See text for additional details.

subsequent oxidation of CHO or COH to CO would be relatively slow, causing some accumulation to occur. Nevertheless, the relatively slow rate of methanol adsorption at low potential means that the coverage of CHO or COH would still be quite low at the short times probed in our experiment. As the potential is increased, CHO or COH accumulates more rapidly, so that Frumkin adsorption of this intermediate begins to slow the rate of methanol adsorption, causing the weak increase in current with potential between 0.35 and 0.52 V. Above 0.52 V, oxidation of CHO or COH to CO becomes fast enough to stabilize the CHO/COH coverage on the experimental time scale, lowering the Tafel slope back to 120 mV decade^{-1}. Although Tafel slopes close to 120 mV decade^{-1} often indicate a process in which the first electron transfer is rate limiting, they are also compatible with a later slow electron-transfer step as long as the preceding electron-transfer steps are completely irreversible and have approximately the same potential dependence. This should be the case for methanol dehydrogenation at 0.52 V and higher, since each step occurs at a potential much higher than the standard potential of 0.02 V for methanol oxidation. Figure 10B shows a comparison of the experimentally measured Tafel slope compared with a simulated Tafel slope for a mechanism in which the first and fourth H abstraction events are the slow steps. In this simulation, the rate of the first H abstraction is $(k_1C_m/S)\exp(-\gamma\theta_{COH,CHO})$, while the rate of the fourth H abstraction is $(k_4/S)\theta_{COH,CHO}$. Parameter values used were $k_1 = 2.9 \times 10^{-6}$ cm s^{-1}, γ = 520 ML^{-1}, and $k_4 = 1.8 \times 10^{15}$ molecules cm^{-2} s^{-1}. The quoted values of k_1 and k_4 represent the values at 0.45 V, while values at other potentials were calculated assuming a Tafel slope of 100 mV decade^{-1} for k_1 and 120 mV decade^{-1} for k_4. The second and third H abstractions were modeled as infinitely fast, and the simulated current at t = 0.1 s was used to calculate the overall Tafel slope, the same as in the experimental Tafel slope determination. Although the approximate nature of the

(42) Hartnig, C.; Spohr, E. *Chem. Phys.* **2005**, *319*, 185.
(43) Lei, H. W.; Suh, S.; Gurau, B.; Workie, B.; Liu, R. X.; Smotkin, E. S. *Electrochim. Acta* **2002**, *47*, 2913.
(44) Wu, G.; Li, L.; Xu, B. Q. *Electrochim. Acta* **2004**, *50*, 1.
(45) Kandoi, S.; Greeley, J.; Sanchez-Castillo, M. A.; Evans, S. T.; Gokhale, A. A.; Dumesic, J. A.; Mavrikakis, M. *Topics Catal.* **2006**, *37*, 17.
(46) Sriramulu, S.; Jarvi, T. D.; Stuve, E. M. *J. Electroanal. Chem.* **1999**, *467*, 132.
(47) Zhu, Y. M.; Uchida, H.; Yajima, T.; Watanabe, M. *Langmuir* **2001**, *17*, 146.
(48) Bagotzky, V. S.; Vassiliev, Y. B.; Khazova, O. A. *J. Electroanal. Chem.* **1977**, *81*, 229.

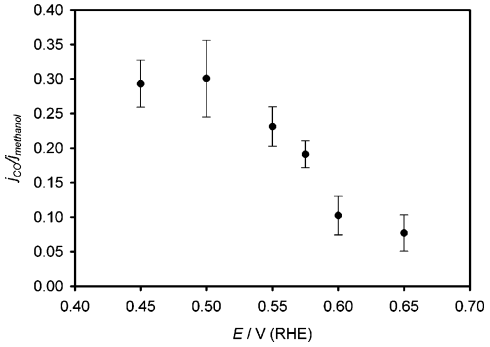

Figure 11. CO oxidation current divided by total methanol oxidation current. See text for experimental details.

simulation results in parameter values that do not necessarily reflect physical values, the ability of the simulation to describe the essential experimental observations indicates that the model is plausible. Thus, we conclude that two of the four H abstraction events during methanol dehydrogenation are much slower than the other two. Although our electrochemical analysis does not allow us to identify the two slow steps, previous reports[23,24,38,43−47] suggest that they are probably the first H abstraction (C−H scission) and the fourth H abstraction (either C−H or O−H scission).

3.4. Invariance of θ_{CO} with Potential. As noted above, the CO coverage increases monotonically with time during methanol oxidation. Although CO formation occurs more rapidly at higher potentials, the steady-state CO coverage on well-ordered Pt(111) is ∼0.28 ML at each potential tested (0.35, 0.45, and 0.55 V) in 0.1 M CH_3OH + 0.1 M NaOH solution. A similar phenomenon was observed as early as the work of Bagotzky et al.[49] The steady-state coverage of 0.28 ML reflects a balance between the rate of methanol decomposition to CO, which decreases with increasing CO coverage, and the rate of oxidative removal of CO, which increases with increasing CO coverage (eq 3). The invariance of steady-state CO coverage with potential stems from the similar potential dependence of methanol dehydrogenation (120 mV decade^{-1}, see above) and CO oxidation (130 mV decade^{-1})[20] in the potential region studied. On the basis of these arguments, the Tafel slope for steady-state methanol oxidation should also be close to 120 mV decade^{-1}. Indeed, the Tafel slope for methanol oxidation between 0.35 and 0.59 V, measured after a potential step to the final potential after generating the steady-state CO coverage at 0.55 V for 30 s, is 110 mV decade^{-1}. This value is in good agreement with the Tafel slope of 120 mV decade^{-1} reported by other workers at slightly higher potential.[32]

3.5. Parallel Pathways. The discussion above assumes that the CO pathway, with carbonate as the final product, is the primary pathway for methanol oxidation. In contrast, previous authors reported low[30] or negligible[32] carbonate formation, with formate as the primary oxidation product.[32] Nevertheless, the results of Figure 11 show that the pathway through CO to carbonate is indeed the primary one during methanol oxidation under our experimental conditions. Oxidation of 0.1 M methanol at 0.45 V was carried out for 400 s to generate a steady-state CO coverage, followed by measurement of the methanol oxidation current at the final potential (between 0.45 and 0.65 V). The solution was then drained and replaced with methanol-free solution, followed by recording of the initial CO oxidation current at the same final potential. Since oxidation of a methanol-generated CO adlayer is indistinguishable from oxidation of CO formed by dosing CO gas (Figure 2), contributions from oxidation of all other adsorbed species may be neglected. The ratio of the CO current and the methanol current measured in this way can be used to assess the relative importance of the CO to carbonate pathway compared with other methanol oxidation pathways. At 0.45 V, the measured CO oxidation current is 29 ± 4% of the methanol oxidation current. This result demonstrates that the CO-to-carbonate pathway accounts for 75−100% of the total methanol oxidation current at 0.45 V. The greater significance of the parallel (formate) pathway found by previous workers may result from the higher potentials used in these studies. For instance, Morallon et al. used FTIR to detect formate as the predominant oxidation product, but the formate band was only measurable at potentials higher than 0.60 V.[30] Indeed, our measurements have revealed a greater significance of the parallel (non-CO) pathway at higher potentials (Figure 11). By 0.65 V, the CO-to-carbonate pathway has decreased to only 20% of the total current. The shift to a parallel pathway at higher potential is also in agreement with results from acidic media in which the parallel pathway on Pt(111) begins around 0.35 V and becomes more significant at higher potential.[26] Still, our observations disagree with reports of significant formate production even at 0.4 V during methanol oxidation on platinized Pt. Indeed, some authors have reported that the CO-to-carbonate pathway becomes more significant with increasing potential,[50] the opposite of what we found. The reason for the discrepancy is unclear, although it may be partly due to differences between rough Pt and smooth Pt(111).

3.6. Role of Defects. Since the steady-state CO coverage is determined by a balance between the rate of methanol dehydrogenation and the rate of CO oxidation (eq 3), accelerating one of these reactions while leaving the other unchanged would shift the steady-state coverage. Such an effect may be realized through the deliberate introduction of a small number of defects on the otherwise well-ordered Pt(111) surface. Lightly disordering a Pt(111) surface in this way has been shown to dramatically accelerate CO oxidation at low potentials, in the "pre-peak" region.[20] The small Pt islands (diameter < 1 nm) formed in the disordering process can provide adsorbed OH at potentials much lower than the onset of OH adsorption on Pt(111) terraces,[20,51,52] while rapid CO diffusion[22,53] allows for transport of CO from terrace sites to defect sites where it can react with defect-bound OH.[20,22] These defects enhance oxidation of pre-peak CO, but the CO pre-peak only develops when the CO coverage is ∼0.20 ML or higher. Below 0.20 ML, CO and defect-bound OH can coexist on the surface with very little reaction.[20] At these lower CO coverage values, oxidation of CO requires terrace-bound OH, so CO oxidation is restricted to the main peak region (potential higher than 0.70 V). Therefore, during methanol oxidation in the potential region examined in this report (0.35−0.55 V), no significant CO oxidation can occur until the CO coverage has reached a value of 0.20 ML. Hence, the current in the early stages of methanol oxidation can be attributed solely to the methanol dehydrogenation reaction (producing CO), and to a small extent (see Figure 11), parallel reaction pathways leading to formate or other dissolved oxidation products without intermediate CO formation. The results of Figure 12 demonstrate that different types of defects have very different effects on methanol dehydrogenation. Methanol oxidation chronoampero-

(49) Bagotzky, V. S.; Vassiliev, Y. B. *Electrochim. Acta* **1966**, *11*, 1439.

(50) Matsuoka, K.; Iriyama, Y.; Abe, T.; Matsuoka, M.; Ogumi, Z. *Electrochim. Acta* **2005**, *51*, 1085.

(51) Teliska, A.; O'Grady, W. E.; Ramaker, D. E. *J. Phys. Chem. B* **2005**, *109*, 8076.

(52) Burke, L. D.; Collins, J. A.; Horgan, M. A.; Hurley, L. M.; O'Mullane, A. P. *Electrochim. Acta* **2000**, *45*, 4127.

(53) Kobayashi, T.; Babu, P. K.; Gancs, L.; Chung, J. H.; Oldfield, E.; Wieckowski, A. *J. Am. Chem. Soc.* **2005**, *127*, 14164.

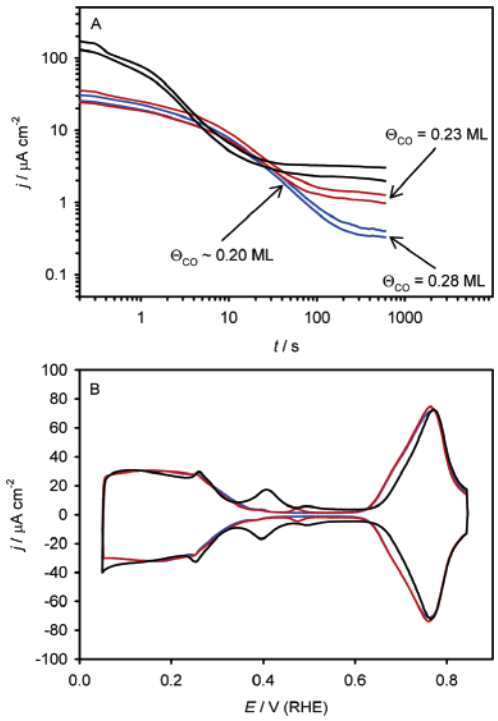

Figure 12. (A) Effect of defects on 0.1 M methanol oxidation at 0.45 V. (B) Background voltammograms representative of the three types of surfaces in (A). Blue line, well-ordered Pt(111); red line, lightly disordered Pt(111), with 0.5−1 nm diameter Pt islands; black line, highly disordered Pt(111), with 1−4 nm diameter Pt islands. Lines in (A) represent 95% confidence bands.

grams for well-ordered Pt(111) and for lightly disordered Pt-(111) are indistinguishable at short times. At 0.45 V, the two traces begin to diverge after ~40 s. The time at which divergence occurs is close to the time required to form 0.20 ML of CO (also ~40 s, see Figure 7). At longer times, the surface with small island defects produces a markedly higher oxidation current, a result that can be understood in the context of the lower steady-state CO coverage on such a lightly disordered surface, 0.23 ± 0.02 ML, as compared with 0.28 ± 0.01 ML for the well-ordered surface. These observations underscore the conclusion that small Pt islands greatly enhance CO oxidation but have no significant effect on methanol dehydrogenation. In contrast, larger Pt islands (diameter 1−4 nm)[20] effectively promote methanol dehydrogenation, as demonstrated by the much higher initial current and more rapid current decay for highly disordered Pt(111) in Figure 12. This difference is due to the different adsorption sites present on large and small Pt islands. Whereas the edges of small islands have adsorption sites with geometry similar to kink sites, large islands are characterized by (110) and (100) oriented step edges.[20] Previous reports have indicated that both kinds of steps promote methanol dehydrogenation,[54−57] in agreement with our observations. Thus, defects with kink-type geometry and defects with step-type geometry appear to have very different effects on methanol dehydrogenation and oxidation. The difference can be understood in the context of geometric vs electronic effects. Electronic perturbations at small Pt islands cause OH adsorption at lower potentials than on terraces and thus accelerate CO oxidation. Step-type defects behave similarly in this respect.[58,59] Although the electronic effect is relevant for complete methanol oxidation via CO, it does not seem to play a large role in methanol dehydrogenation, since only step-type defects are active in promoting this reaction (Figure 12, cf. ref 33). Therefore, we conclude that adsorbed OH does not play a significant role in methanol dehydrogenation. This is not surprising since Pt is known to be an efficient catalyst for C−H bond cleavage[24,60−62] and since H can readily desorb from Pt without any need for adsorbed OH.[63] Rather, the local geometry at (110) and (100) steps is responsible for their high activity. Both Pt(110) and Pt(100) are known to be much more active than Pt(111) for methanol dehydrogenation,[25] so it appears that (110) and (100) steps on Pt(111) act simply as small Pt(110) and Pt(100) domains.

3.7. Accelerating Methanol Oxidation. Since the rate of methanol oxidation decreases as the CO coverage increases, a clear path toward improved catalytic efficiency is to lower the steady-state CO coverage. This can be achieved in part by introducing Pt sites that are more capable of supplying adsorbed OH, namely, defect sites, but even this approach only lowers the steady-state CO coverage slightly. On the Pt(111) surface, the lowest steady-state CO coverage that could be hoped for using this method is ~0.20 ML. Below this coverage, voltammetric CO oxidation produces no pre-peak,[20] indicating that CO oxidation is extremely slow in the potential region of interest for DMFC anodes when the CO coverage is low. A similar conclusion may be drawn from the exponential dependence of the CO oxidation rate on CO coverage (Figure 8A). The reason for the 0.20 ML minimum coverage on defective Pt(111) surfaces lies in the coverage-dependent adsorption energy of CO. The Pt−CO bond becomes markedly stronger at low CO coverage,[64,65] such that for $\theta_{CO} < 0.20$ ML the defect-bound OH species is not sufficiently reactive to oxidize the extremely stable low-coverage CO. One approach to removing CO, even at low potential and CO coverage, is to provide additional adsorbed OH by addition of a second, more oxophilic metal, such as Ru,[66] which can promote CO oxidation via a bifunctional mechanism.[67] Conceivably, the OH species adsorbed on Ru or other promoters may be more active for CO oxidation than OH adsorbed on Pt defects. Although the ability of Ru to promote methanol oxidation on Pt(111) in acid electrolytes is notable,[68,69] in alkaline electrolytes the effect is much weaker,[21] presumably because the OH species adsorbed on Ru sites is still too strongly bound to be sufficiently reactive with adsorbed CO on Pt sites. Weakening the Pt−CO bond via a change in Pt electronic structure[70−72] presents another path toward improved methanol oxidation activity. On a Pt surface in which the electronic structure has been altered in such a way

(54) Shin, J. W.; Korzeniewski, C. *J. Phys. Chem.* **1995**, *99*, 3419.
(55) Housmans, T. H. M.; Koper, M. T. M. *J. Phys. Chem. B* **2003**, *107*, 8557.
(56) Desai, S. K.; Neurock, M.; Kourtakis, K. *J. Phys. Chem. B* **2002**, *106*, 2559.
(57) Gibson, K. D.; Dubois, L. H. *Surf. Sci.* **1990**, *233*, 59.
(58) Lebedeva, N. P.; Rodes, A.; Feliu, J. M.; Koper, M. T. M.; van Santen, R. A. *J. Phys. Chem. B* **2002**, *106*, 9863.
(59) Lebedeva, N. P.; Koper, M. T. M.; Feliu, J. M.; van Santen, R. A. *J. Phys. Chem. B* **2002**, *106*, 12938.
(60) Sexton, B. A. *Surf. Sci.* **1981**, *102*, 271.
(61) Waszczuk, P.; Lu, G. Q.; Wieckowski, A.; Lu, C.; Rice, C.; Masel, R. I. *Electrochim. Acta* **2002**, *47*, 3637.
(62) Diekhoner, L.; Butler, D. A.; Baurichter, A.; Luntz, A. C. *Surf. Sci.* **1998**, *409*, 384.
(63) Conway, B. E. Electrochemical Processes Involving H Adsorbed at Metal Electrode Surfaces. In *Interfacial Electrochemistry*; Wieckowski, A., Ed.; Marcel Dekker: New York, 1999; p 131.
(64) Ertl, G.; Neumann, M.; Streit, K. M. *Surf. Sci.* **1977**, *64*, 393.
(65) Yeo, Y. Y.; Vattuone, L.; King, D. A. *J. Chem. Phys.* **1997**, *106*, 392.
(66) Spendelow, J. S.; Wieckowski, A. *Phys. Chem. Chem. Phys.* **2004**, *6*, 5094.
(67) Maillard, F.; Lu, G. Q.; Wieckowski, A.; Stimming, U. *J. Phys. Chem. B* **2005**, *109*, 16230.
(68) Gasteiger, H. A.; Markovic, N.; Ross, P. N.; Cairns, E. J. *J. Phys. Chem.* **1993**, *97*, 12020.
(69) Chrzanowski, W.; Wieckowski, A. *Langmuir* **1998**, *14*, 1967.
(70) Hammer, B.; Morikawa, Y.; Norskov, J. K. *Phys. Rev. Lett.* **1996**, *76*, 2141.
(71) Tong, Y. Y.; Kim, H. S.; Babu, P. K.; Waszczuk, P.; Wieckowski, A.; Oldfield, E. *J. Am. Chem. Soc.* **2002**, *124*, 468.
(72) Lu, C.; Masel, R. I. *J. Phys. Chem. B* **2001**, *105*, 9793.

as to weaken the Pt−CO bond, adsorbed OH species could remain active for CO oxidation at lower CO coverage than on an unmodified Pt surface, thus allowing for a decrease in the steady-state CO coverage during methanol oxidation. Although the exact method of achieving such an electronic effect is yet to be determined, recent theoretical[70,73−75] and experimental[75−78] advances in the understanding of the effects of strain and charge transfer on electronic structure present a path toward altering electronic structure in order to optimize catalytic activity.

4. Summary and Conclusions

Despite previous reports of very low CO coverage during methanol oxidation on Pt(111) in alkaline media, the results of this study demonstrate that CO poisoning is the most significant cause of the current decay during methanol oxidation. At DMFC-relevant potentials, most methanol oxidation occurs through the CO pathway, leading to carbonate as the final product. Parallel (non-CO) pathways, with formate as a likely final product, become more significant at potentials higher than 0.5 V.

The rate of methanol dehydrogenation is limited by repulsive interactions between CO and methanol dehydrogenation intermediates, leading to Elovich-type CO accumulation. The rate of CO oxidation is also dominated by adsorbate−adsorbate interactions, leading to an exponential dependence of CO oxidation rate on CO coverage. The steady-state CO coverage, which is ∼0.28 ML in 0.1 M methanol solutions, results from a balance between the rate of methanol dehydrogenation and the rate of CO oxidation. This steady-state coverage does not change significantly with potential in the range 0.35 −0.55 V, since the rates of methanol dehydrogenation and CO oxidation have almost the same potential dependence.

Different types of defects have different roles in methanol oxidation. Small islands, with kink-type adsorption sites, strongly promote CO oxidation but have no effect on methanol dehydrogenation. Large islands, with step-type adsorption sites, promote methanol dehydrogenation and CO oxidation. In promoting methanol dehydrogenation, steps seem to be active more because of the geometric arrangement of surface atoms, (100) or (110), than because of any electronic perturbations associated with these defects. In contrast, the electronic perturbations at very small Pt islands, which lead to OH adsorption at much lower potential than on terraces, are responsible for the high CO oxidation activity at these defects. Pt(111) terraces are moderately active for methanol dehydrogenation but have virtually no activity for CO oxidation at potentials of interest for DMFCs. Therefore, the rate of steady-state methanol oxidation even on highly ordered Pt(111) is controlled by the defect density.

Since the rate of methanol dehydrogenation is severely decreased by CO, lowering the CO coverage is an obvious method to improve catalytic performance. Nevertheless, the ability of CO to decelerate methanol dehydrogenation even at very low CO coverage complicates this strategy, since in the potential range of interest significant CO oxidation only occurs when $\theta_{CO} > 0.20$ ML. Below this coverage, CO is too strongly bound to react with coadsorbed OH (on defects). Therefore, a promising route toward increased methanol oxidation activity is to decrease the Pt−CO bond strength, an effect that could conceivably be achieved by exploiting strain and charge-transfer effects with appropriately selected substrates and alloying components. For instance, the Pt−CO bond is known to be weakened when Pt is alloyed with or deposited as a monolayer on top of a metal with a smaller lattice constant, such as Ru or Ni.[74] The Pt−CO bond is also weakened by the presence of a second metal, such as Ru, which withdraws electron density from Pt sites.[71,79] Alternatively, promotion of methanol dehydrogenation, even in the presence of CO, is also a promising route toward enhanced methanol oxidation. As will be reported soon,[21] the electronic effects caused by adding Ru to a Pt(111) surface can promote methanol dehydrogenation, while at the same time decreasing the influence of CO on this reaction.

Although the present study is devoted to methanol oxidation on highly idealized Pt surfaces (as compared with those used in technical catalysts), we believe that the understanding of fundamental mechanisms and limiting factors in methanol oxidation, with resulting identification of possible approaches to improving catalytic activity, will be useful in the development of more active DMFC anode electrocatalysts. In particular, the examination of similarities and differences between electrocatalytic mechanisms in alkaline and acidic media is important for the design of alkaline DMFCs, including the LFFC, which shows much promise as a fuel cell platform capable of operating with electrolytes of any pH value.[11]

Acknowledgment. This work is supported by the NSF under Grant No. CHE 03-49999 and by the DOE under Grant No. DE-FG02005ER46260. Part of this work was supported by a CAREER award from NSF-CTS to P.J.A.K. J.S.S. acknowledges support from a NSF Graduate Research Fellowship.

LA0615995

(73) Mavrikakis, M.; Hammer, B.; Norskov, J. K. *Phys. Rev. Lett.* **1998**, *81*, 2819.
(74) Shubina, T. E.; Koper, M. T. M. *Electrochim. Acta* **2002**, *47*, 3621.
(75) Schlapka, A.; Lischka, M.; Gross, A.; Kasberger, U.; Jakob, P. *Phys. Rev. Lett.* **2003**, *91*.
(76) Kibler, L. A.; El-Aziz, A. M.; Hoyer, R.; Kolb, D. M. *Angew. Chem., Int. Ed.* **2005**, *44*, 2080.
(77) Hager, T.; Rauscher, H.; Behm, R. J. *Surf. Sci.* **2004**, *558*, 181.
(78) Zhang, J.; Lima, F. H. B.; Shao, M. H.; Sasaki, K.; Wang, J. X.; Hanson, J.; Adzic, R. R. *J. Phys. Chem. B* **2005**, *109*, 22701.
(79) Spendelow, J. S.; Babu, P. K.; Wieckowski, A. *Current Opin. Solid State Mater. Sci.* **2005**, *9*, 37.